On residual stress development during gaseous nitriding of M2 steel

Yanxue Zhang, Sébastien Jégou, Laurent Barrallier, David Mercs

On residual stress development during gaseous nitriding of M2 steel

Yanxue Zhang[a,b,*], Sébastien Jégou[a], Laurent Barrallier[a] and David Mercs[b]

[a]*MSMP laboratory, Arts et Metiers Institute of Technology, 2 cours des Arts et Métiers, 13617, Aix-en-Provence, France.*
[b]*Department of Research Innovation Expertise, Lisi-automotive, 2 rue Juvénal VIELLARD, 90600, Grandvillars, France.*

ABSTRACT

The evolution of residual stress is strongly dependent on chemical and thermodynamic reactions during gas nitriding with respect to phase transformations. This study presents and analyzes the residual stress profiles in M2 high speed steel samples with different gas nitriding parameters (temperatures, times, nitriding potentials). The relationships between residual stress, hardness and corresponding chemical composition profiles are investigated.

Keywords: Residual stress, Phase transformation, Gaseous nitriding, M2 steel, Hardness

1. Introduction

High-speed steels are always subjected to high pressure or high shear working conditions as forming tools, high hardness and compressive residual stresses are required to improve the wear resistance and fatigue life of the tools [1-3]. Nitriding is a thermochemical treatment based on the diffusion of nitrogen that is often used to modify the mechanical properties in the surface layer [4]. The hardness gradient in the nitriding layer is generally consistent with the nitrogen concentration gradient, of which the maximum is at the surface [5]. But the residual stress evolution is more complicated during nitriding, the maximum value is often at depth due to carbon redistribution and precipitate coarsening [6]. Therefore, it is very important to understand how the residual stress evolves in the material during nitriding to obtain an optimized mechanical profile.
Origins of residual stresses during nitriding have been attributed to volume changes caused by nitride precipitation and phase transformations of initial carbides [1,4,7]. An in-depth gradient of residual stresses develops below the surface with the compositional gradient. In the case of M2 steel, the alloying elements (Cr, Mo, V, W) form nitrides with nitrogen diffused in the material and participate in phase transformations between the carbides and nitrides [3]. The

* Corresponding author. yanxue.zhang@ensam.eu

transformation of carbides and the co-diffusion of carbon decrease nitriding kinetics and have an impact on the residual stress [6,8].

2. Experiments

2.1. Material and sample preparation

AISI M2 steel was hardened and tempered with a final hardness of 763 ± 35 HV0.2. The chemical composition was measured as shown in Table 1. Samples with dimensions 17×13×5 mm^3 were nitrided in a thermogravimetric analyzer Setsys Evo ATG-ATD/DSC from SETARAM Instrumentations. The nitriding temperatures are 500 and 540 °C, nitriding potential varies from 0.5 to 3.7 $atm^{-1/2}$, and the nitriding time is from 5 hours to 15 hours.

Table 1: Chemical composition of M2 steel samples (wt.%).

C	W	Mo	V	Cr	Si	Co	Mn	N
0.884	6.352	4.513	1.729	3.807	0.306	0.372	0.271	0.025

2.2. Characterization methods

A JEOL 7001F microscope, equipped with an Oxford Instrument INCA energy-dispersive X-ray detection system (EDX) has been used for observation and local chemical analysis. Back-scattered electrons (BSE) mode with EDX technic was applied for phase analysis. The observation was performed with an accelerating voltage of 12 kV.

The concentrations of nitrogen and carbon were measured using an optical emission spectrometer Spectromax BT MX5M from Ametek. The in-depth concentration analyses are carried out by successive measurements at depths reached by grinding with a SiC disk of 120 grade to remove about 25 µm thickness after each series of measurements. The result gives the mean value of all the removed material of four tests at each depth.

The micro-hardness was measured with Q10A+ from Qness indentation device with the help of the programming function of the software QpixControl2. A load of 2 N was applied for 10 seconds. Three tests were performed at each equivalent area on a mirror-polished surface.

The residual stress analyses were performed on a Siemens D500 diffractometer, equipped with a linear detector from Elphyse, a chromium anode $\lambda_{k\alpha} = 0.2291$ nm and a vanadium filter. The $\sin^2\psi$ method was used for stress calculation on the {211} family planes of ferrite. The analysis is performed using 13 ψ angles, including an oscillation of +/− 3° and an acquisition time of 100 s. The X-ray elastic constant were calculated from ferrite elasticity constants (Young modulus E = 210 GPa, Poisson ratio ν = 0.29, anisotropy factor ARX = 1.39) and Kröner-Eshelby type model ($1/2\ S_2 = 5.81\times10^{-6}\ MPa^{-1}$, $S_1 = -1.27\times10^{-6}\ MPa^{-1}$). The in-depth profile below the surface was reached by successive electrochemical polishing (Struers Lectropol 5, with electrolyte A2) using a depth increment of nearly 20 µm controlled by an electronic micrometer.

3. Results and discussions

3.1. Nitriding time

Fig.1. (a) shows the chemical profiles of nitrogen and carbon from the surfaces to in-depths of the three samples nitrided for 5 and 15 hours respectively at 500 °C with a nitriding potential

$K_N = 1\ atm^{-1/2}$. As the nitriding time increases, nitrogen diffuses deeper. The maximum nitrogen concentration near the surface is about the same for all the tree samples. Carbon accumulates at the nitrogen diffusion front, as shown by the plateau in the carbon concentration curve. This accumulation allows the formation of the alloy carbides, which can transform into alloy nitrides and grain boundary (GB) cementite during nitrogen diffusion. The plateau extends over 100 µm. According to the depth of GB nitrides and the onset of GB cementite, they are located at relatively higher nitrogen concentrations. Near the surface, decarburization is observed. The longer the nitriding, the more carbon leaves the surface. As shown in Fig.1. (a), the carbon concentration curve for the sample nitrided for 15 hours shows a lower value at the surface than the other sample nitrided for a shorter time.

Fig.1. (b) illustrates the hardness profiles of these three samples. The effective nitriding depth increases as the nitriding time increases, however, the maximum hardness at the surface does not change much. This is because the hardening is related to the precipitation of alloying elements nitrides MN (M=Cr, V, Mo...), which are finely dispersed into the ferritic matrix, and thus to the content and diffusion of nitrogen through the treated surface [9], especially in the diffusion zone. Accordingly, the deeper the diffusion into the steel over a longer nitriding period, the greater the effective nitriding depth presents in the hardness profile. The nitrogen concentration reaches the same limit due to the concentration of alloying element in the material, as does the amount of nitride precipitates. Thus, the maximum hardness increase with the same value despite the different nitriding parameters.

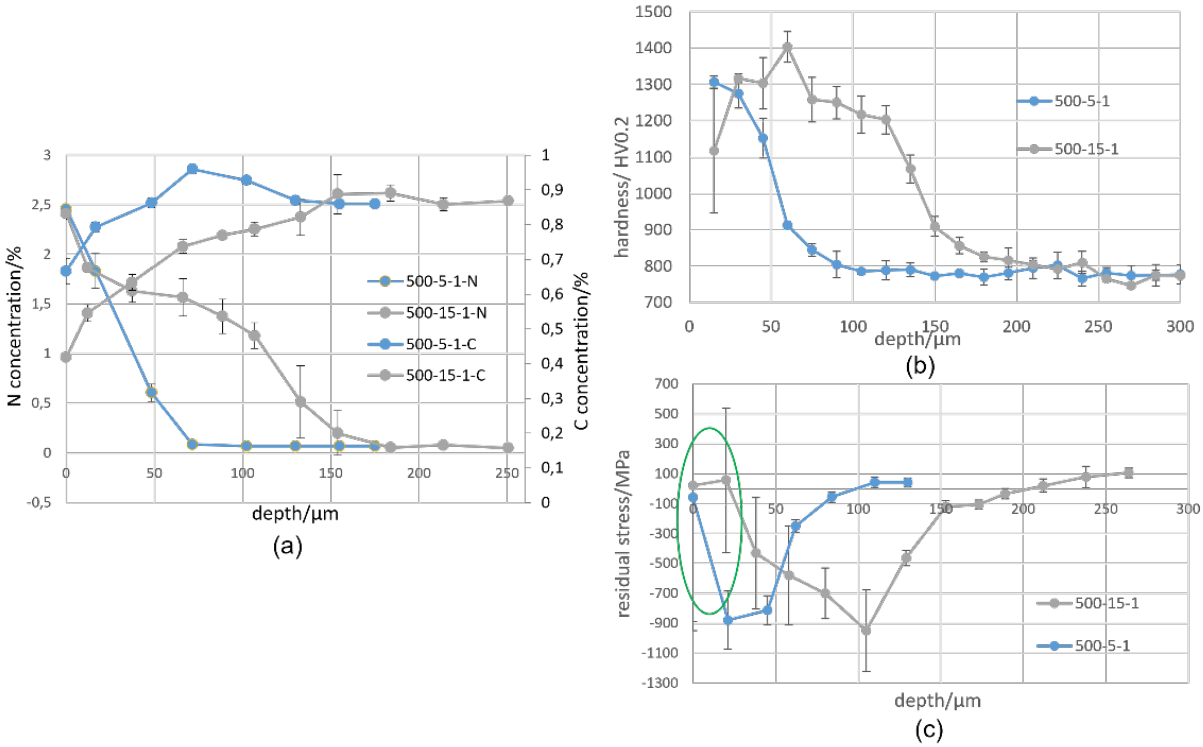

Fig. 1. Surface to an in-depth profile of M2 steel after gas nitriding at 500 °C for 5 and 15 hours with nitriding potential of $K_N = 1\ atm^{-1/2}$ (a) N, C profile, (b) hardness profile, (c) residual stress.

The compressive residual stresses are generated due to the positive volumetric eigenstrains accompanying the precipitation of alloying elements nitrides within the ferritic matrix. MN nitrides (M=Cr, V...) are characterized by a higher specific volume than the ferritic matrix (10.7 and 7.1 $cm^3mol^{-1,}$ respectively) [8,9]. The volume expansion varies depending on the nitrogen fraction. In Fig.1. (c), the maximum compressive residual stress shifts to a greater depth after longer nitriding. Comparing with Fig.1. (a), the maximum residual stress is located just before

the carbon plateau. This means that the maximum residual stress occurs just after the carbon concentration returns to the normal value for the studied M2 steel, accompanied by a transformation of carbides to nitrides at a particular depth. From the phase aspect, all alloying elements transform into alloy nitrides at the depth where the residual stresses reach the maximum value. The transformation of initial carbides into nitrides decreases nitriding kinetics and is counteracted by cementite precipitation. This reduces the volume change and thus the residual stresses during nitriding. During nitriding, the evolution of precipitation and phase transformation consists of four steps [9].

• MN nitride precipitation occurs at the beginning of the treatment or diffusion of nitrogen atoms. Due to the high nitrogen affinity, fine semi-coherent MN nitrides precipitate from the solid solution and generate compressive residual stress.

• The transformation from initial carbides to incoherent nitrides offers less volume change due to a minor specific volume difference.

• Diffusion of carbon at the diffusion front react with alloying elements to form carbides first, then transform to incoherent nitrides, resulting in a lower quantity of semi-coherent nitrides and less volume expansion at a deeper depth.

• The transformation from cementite to iron nitrides accompanied by carbon diffusion causes decarburization close to the surface, which decreases the elastic loading induced by the former phase transformations during nitriding.

The first three steps all lead to an increase in volume and compressive residual stress, with a different ratio. At greater depths, the second and third types of phase transformations occur more significantly [10], leading to a decrease in the number of alloying elements joining the first type of phase transformation, resulting in a relatively smaller volume expansion. Hence, when the maximum compressive residual stress occurs in the deeper material, the value is generally lower than those near the surface. Once the maximum residual stress is reached, similar to the effect of aging time on the size of the precipitates, further nitriding leads to precipitates coarsening and redistribution of residual stress [11,12]. Surface decarburization involves a reduction in the volume fraction of precipitates during nitriding, resulting in unloading at the surface and thus a decrease of compressive residual stress [8]. Positive residual stress can even be generated depending on the kinetics of phase transformations during nitriding (Fig.1. (c) 15 hours nitriding).

3.2. Nitriding temperature

Fig.2. shows the profiles of chemical and mechanical properties from the surface to in-depths of the M2 samples after nitriding with $K_N = 0.5\ atm^{-1/2}$ at 500 and 540 °C. For the nitrogen and hardness profiles, the values reach the maximum at the surface and gradually decrease until they are identical to those in the core. Nitriding at a lower temperature (500 °C) leads to a less significant increase in hardness and a lower nitriding depth, as shown in Fig.2.(c). This corresponds to less nitrogen diffusion leading to a low nitrides fraction, as shown in Fig.2. (a), a lower nitrogen concentration in the material from the surface to in-depth compared to that nitrided at 540 °C. After carbon enrichment at a certain depth, the carbides transform into nitrides and cementite precipitate at the grain boundaries. Where the phase composition allows for maximum volume expansion, and the maximum residual stress occurs. By increasing the nitriding temperature, the nitriding layer grows faster, and the maximum residual stress occurs at a greater depth below the surface. In Fig.2. (b), the residual stress shows the highest value at the surface of the sample nitrided at 500 °C, while at about 50 µm in-depth of the sample

nitrided at 540 °C due to the residual stress redistribution. The lower carbon concentration of the sample nitrided at 540 °C (Fig.2. (a)) indicates a more critical decarburization.

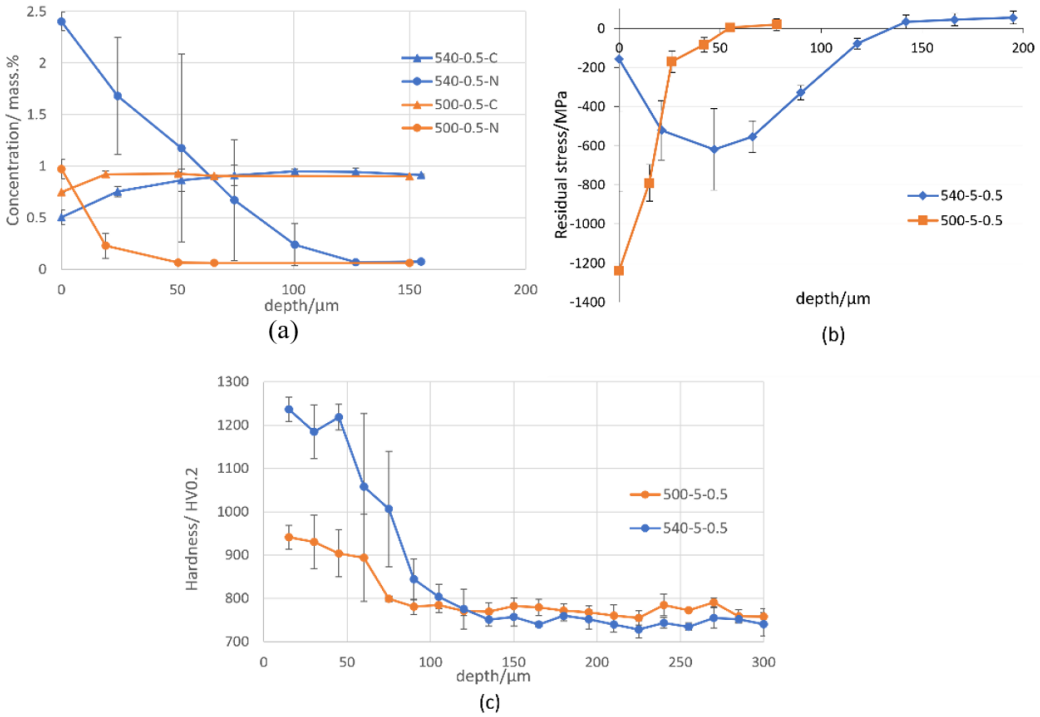

Fig. 2. Surface to an in-depth profile of M2 steel after gas nitriding with $K_N = 0.5$ atm$^{-1/2}$ at different temperatures (a) N, C profile, (b)residual stress, (c)hardness profile.

3.3. Nitriding potential

The N/C concentration profiles, the hardness profiles, and the residual stress profiles in M2 steel samples after gas nitriding at 540 °C are shown in Fig.3. A compound layer is formed with a nitriding potential of $K_N = 3.7$ atm$^{-1/2}$, but no compound layer was observed for $K_N = 0.5$ atm$^{-1/2}$. The effective nitriding depth is greater for $K_N = 3.7$ atm$^{-1/2}$, as is the depth of the maximum residual stress. This results from the more pronounced nitrides precipitation since the nitrogen concentration is higher in the sample nitrided with $K_N = 3.7$ atm$^{-1/2}$. A higher nitriding potential increases the decomposition of ammonia and provides a higher fraction of nitrogen atoms at the gas-solid interface. This changes the boundary condition of the diffusion. The low residual stress and low carbon concentration near the surface are due to the decarburization and carbon redistribution (carbide transformation and carbon co-diffusion), as explained earlier.

4. Conclusion

A nitrogen concentration gradient is generated during nitriding through the surface of the treated part. The hardness gradient is consistent with the nitrogen concentration. The maximum residual stress is generally located at the end of the hardness plateau before the nitrogen diffusion front. At deeper depths, carbon accumulation can be observed. The maximum residual stress occurs after the transformation of carbides to alloy nitrides and the co-diffusion of carbon. However, the residual stress redistributes when nitriding is longer due to multiple phase transformations, precipitates coarsening, and decarburization at the surface.

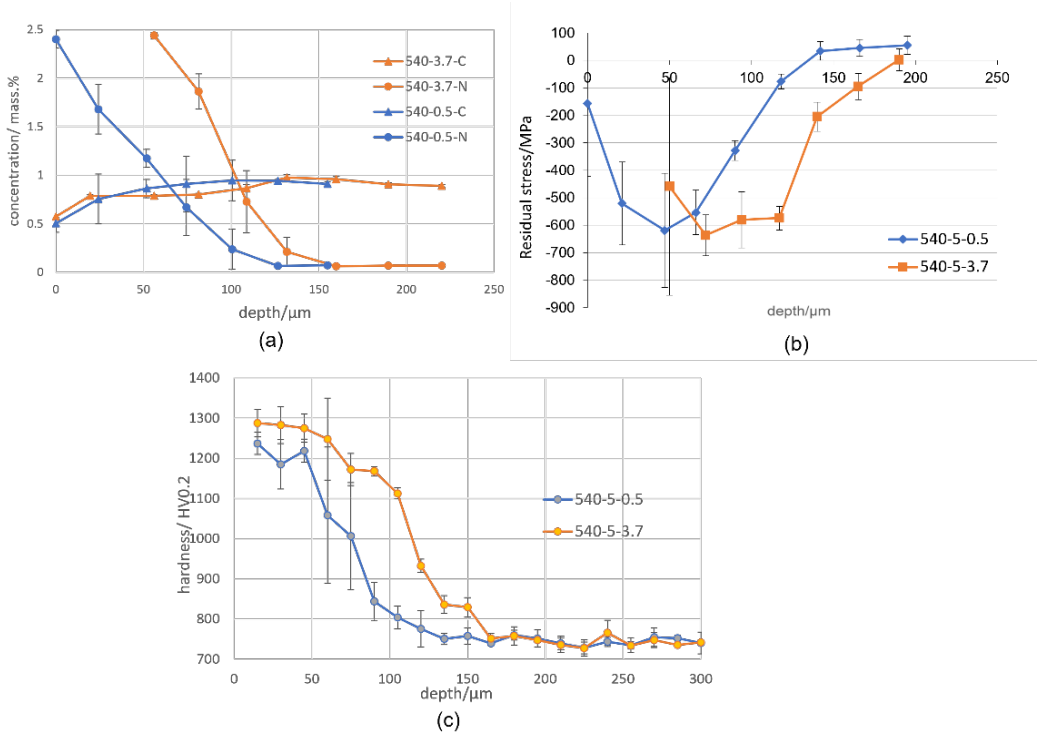

Fig. 3. Surface to an in-depth profile of M2 steel after gas nitriding at 540 °C with different nitriding potential (a) N, C profile, (b)residual stress, (c)hardness profile.

References

[1] L.H.P. Abreu, M.C.L. Pimentel, W.F.A. Borges, T.H.C. Costa, M. Naeem, J. Iqbal, and R.R.M. Sousa. Plasma nitriding of AISI M2 steel: performance evaluation in forming tools. Surface Engineering, p.1-8, 2020.

[2] I. Hacisalihoglu, F. Yildiz, and A. Alsaran. Wear performance of different nitride-based coatings on plasma nitrided AISI M2 tool steel in dry and lubricated conditions. Wear, 384(2017)159-168.

[3] R. Mohammadzadeh, A. Akbari, and M. Drouet. Microstructure and wear properties of AISI M2 tool steel on RF plasma nitriding at different N_2-H_2 gas compositions. Surface and Coatings Technology, 258(2014)566-573.

[4] E.J. Mittemeijer, Fundamentals of nitriding and nitrocarburizing, ASM International, 153(2013)619–646.

[5] E.J. Mittemeijer and M.A.J. Somers. Thermodynamics, kinetics, and process control of nitriding. Surface Engineering, 13(6):483–497, 1997.

[6] S. Jégou, R. Kubler and L. Barrallier, On residual stresses development during nitriding of steel: thermochemical and time dependence, Advanced Materials Research Vols. 89-91 (2010) pp 256-261

[7] L. Barrallier, J. Barrallis, On origin of residual stresses generated by nitriding treatment on alloy steel. Proc. 4th Int. Conf. Residual Stress, Baltimore. (1994), p.498-505

[8] S. Jégou, L. Barrallier, and G. Fallot, Gaseous nitriding behavior of 33CrMoV12-9 steel: Evolution of the grain boundaries precipitation and influence on residual stress development. Surface and Coatings Technology, 339(2018)78–90.

[9] S. Jegou, L. Barrallier, and R. Kubler. Phase transformations and induced volume changes in a nitrided ternary Fe–3%Cr–0.345%C alloy. Acta Materialia, 58(7):2666– 2676, 2010.

[10] S. Jegou, L. Barrallier, R. Kubler, and M.A.J. Somers. Evolution of residual stress in the diffusion zone of a model Fe-Cr-C alloy during nitriding. HTM Journal of Heat Treatment and Materials, 66(3):135–142, 2011.

[11] Van Landeghem, P. Hugo, M. Gouné, and A. Redjaïmia, (2012). Nitride precipitation is compositionally heterogeneous alloys: Nucleation, growth, and coarsening during nitriding. *Journal of crystal growth*, *341*(1), 53-60.
[12] T. Steiner, M. Akhlaghi, S.R. Meka, and E.J. Mittemeijer, (2015). Diffraction-line shifts and broadenings in continuously and discontinuously coarsening precipitate-matrix systems: coarsening of initially coherent nitride precipitates in a ferrite matrix. *Journal of materials science*, *50*(21), 7075-7086.